Uncertainty of solar radiation in urban canyons propagates to indoor thermo-visual comfort

Author:
MeshkinKiya, M; Paolini, R

Publication details:
Solar Energy
v. 221
pp. 545 - 558
0038-092X (ISSN); 1471-1257 (ISSN)

Publication Date:
2021-06-01

Publisher DOI:
https://doi.org/10.1016/j.solener.2021.04.033

Uncertainty of Solar Radiation in Urban Canyons Propagates to Indoor Thermo-Visual Comfort

Maryam MeshkinKiya[a],[*] Riccardo Paolini[b]

[a] Department of Architecture, Built environment and Construction engineering, Politecnico di Milano, Milan, Italy

[b] School of Built Environment, University of New South Wales, Sydney, NSW, Australia

Accepted for publication in Solar Energy
https://doi.org/10.1016/j.solener.2021.04.033

Abstract

The incident solar radiation on building facades is strongly affected by the urban characteristics, however frequently overlooked in the assessment of indoor environments due to limited data availability. Here, we show that a simplified representation of the urban environment can drastically affect the estimation of the incident solar radiation within urban canyons. We associate uncertainties with the canyon's geometry, built surfaces, optical properties, as well as vegetation, and resort to a hybrid probabilistic-possibilistic approach to quantify the effects on thermo-visual comfort. Contrasting complex against simplified urban canyons shows that the pattern of incident solar radiation is uneven along the building façade and strongly correlated to the canyon's characteristics. We also demonstrate that simplified models of urban canyons could underestimate the number of thermally comfortable instances by even 365 hours a year (i.e., ~ 4% of the time). Similarly, a simplified canyon underestimates the visually comfortable occurrences, especially during the intermediate seasons. While a simplified canyon estimates a glare probability of 1.0, uncertainties within a complex canyon can lower the glare probability to 0.28 throughout the day. We show that for visual comfort, geometric characteristics alone, such as the canyon's skyline, can outweigh optical properties such as the transmittance of trees. This uncertainty, especially in the estimate of glare probability, may lead to different decisions about building envelope design, including the need for a more or less adaptable façade.

Keywords: Urban canyon, Solar radiation, Uncertainty, Thermal comfort, Visual comfort

Nomenclature

Abbreviation

MRT	Mean Radiant Temperature (°C)
PMV	Predicted Mean thermal sensation Vote (d.u.)
WWR	Window to Wall Ratio (d.u.)
DGP	Daylight Glare Probability (d.u.)

Symbol

f_{eff}	Fraction of occupant body which is directly affected by solar radiation inside the building (d.u.)
h_r	Radiant heat transfer coefficient (W m^{-2} K^{-1})
T_a	Indoor air temperature (°C)
$\propto_{Sw}$	Shortwave absorptivity (d.u.)
$\propto_{Lw}$	Longwave emissivity/ absorptivity (d.u.)
T_{sol}	Window solar transmittance (d.u.)
A_D	Body surface area (m^2)
A_p	Projected area of the human body exposed to direct beam radiation (m^2)
f_{svv}	Fraction of the sky that affects the occupant activities (d.u.)
f_p	Projected area factor (d.u.)
$SunAzimuth_h$	Hourly sun azimuth angle (°)
$SunAltitude_h$	Hourly sun altitude angle (°)
h	Hour
I_{diff}	Hourly diffuse solar radiation (W m^{-2})
I_{global}	Hourly global solar radiation (W m^{-2})
I_{dir}	Hourly direct solar radiation (W m^{-2})
R_{floor}	Reflectance of the floor (d.u.)
Trans	Transmissivity (d.u.)

1. Introduction

The combination of global climate change and increased remote working, and homeschooling driven by the COVID-19 pandemic are leading people to spend increasingly more time indoors, which results in an increased expectation of thermal comfort. Providing comfort for occupants

while reducing energy consumption is essential for current and future sustainable design (Ren and Chen, 2018), given that people's productivity is strongly correlated with the quality of the indoor environment (Al Horr et al., 2016). For instance, exceeding the thermal comfort limit by 1 °C reduces the workers' productivity by 2 % (Mujan et al., 2019). Since the tertiary sector employees spend most of their working hours in offices, comfort in office buildings is crucial to their performance (Antoniadou and Papadopoulos, 2017). Concerning office buildings, the simultaneous thermal and visual comfort assessment is one of the ongoing research lines (Ozcelik et al., 2019; Teixeira et al., 2020), disentangling the mutual influences (Costanzo and Donn, 2017). There is also a greater availability of longitudinal data and, as their spatiotemporal resolution increases, the link between outdoor environments and occupants' responses becomes clearer (Gronlund and Berrocal, 2020), which is critical for understanding and quantifying occupants' comfort (Yang et al., 2020).

Multisensory investigation of indoor comfort showed that the selection of physical factors is core to a proper audit of the indoor environment (Yang and Moon, 2019) and that the simultaneous consideration of ventilation, thermal, and luminous autonomy comfort metrics can affect design decisions (Ko et al., 2018). Simultaneous thermal and visual comfort (thermo-visual comfort) is achieved by various means, as suggested by adjusting the configuration of windows (Zomorodian and Tahsildoost, 2017). The importance of combing different comfort metrics is proved by experiments as well. For instance, the occupants' exposure to higher daylight availability affects their thermal sensation, with greater satisfaction in indoor environments with high daylight availability, even if the indoor temperature is below the conventional values (Chinazzo et al., 2019). Meanwhile, different genders perceive thermal comfort dissimilarly when exposed to shortwave solar radiation (Yang et al., 2020). Satisfying thermo-visual comfort can be extremely challenging when operating shading systems, as meeting one criterion (visual comfort) can exceed the threshold of the other (thermal comfort) (Kristl et al., 2008). In such cases, detailed information on both comfort metrics is vital for automated and movable shading systems to satisfy thermo-visual comfort (Nundy and Ghosh, 2020)(Gong et al., 2019).

1.1 Solar radiation in urban canyon

Despite the complexities, urban canyons are often considered as simple layouts composed of two box-shaped blocks, which is an understandable simplification at the early stages of the development of this type of models or for urban climate modelling. This simplification is reported as one of the possible sources of the building performance gap (Lauzet et al., 2019). In a typical urban canyon model, identical optical properties are considered for all adjacent buildings' exterior surfaces. However, diversity in reflectance and emittance of urban areas (Kotthaus et al., 2014) can be one of the primary sources of uncertainty in the building's surface temperature (Stagakis et al., 2019). Moreover, the canyon's light reflectance affects the level of daylight autonomy in buildings. The reflectance of external walls is a function of the morphology of the façade, which is related to the buildings type (e.g., residential or office), and therefore, it can significantly vary based on the WWR and the chosen façade material. In identical indoor layouts, a high reflectance wall in the canyon (0.75, dimensionless) can eliminate the need for artificial lighting when compared to a low reflectance wall (0.45) (Strømann-Andersen and Sattrup, 2011). Besides material characteristics, geometric features, namely urban layout, can significantly affect solar availability (Martins et al., 2016). In a real urban environment, the vertical and horizontal view factors vary along with its elongation (Svensson, 2004). Trees intercept the shortwave radiation in

several vertical layers inside a canyon, which vary up to 30 %, depending on the time and density of trees (Krayenhoff et al., 2020). The shadowing effect of trees' canopy can reduce the exterior wall temperature by 9 °C (Berry et al., 2013). Including the multi-layer impact of trees within the canyon is suggested for accurate building energy modelling (Krayenhoff et al., 2020).

Solar radiation is among the few factors that simultaneously affect thermal and visual comfort (Ulpiani et al., 2017). Like other urban microclimate features, solar radiation is associated with uncertainty, which becomes more significant when the area of study scales down to the urban canyons (Sun et al., 2014). Given such strong interactions between urban characteristics and solar radiation (Tsoka et al., 2018), studying the uncertainties embedded in an urban canyon is crucial. Nonetheless, due to inadequate measurements for quantifying the complexities of urban canyon features, their impact on the estimation of incident solar radiation is rarely discussed (Nevat et al., 2020). From a macro perspective, aspect ratio and orientation are the fundamental parameters to determine the solar availability within the urban canyons. Smaller aspect ratios and east to west elongations can individually elevate solar availability, yet, a combination of both creates the most stressful conditions for thermal comfort in pedestrian areas (Ali-Toudert and Mayer, 2006; Chatzidimitriou and Yannas, 2017; Krüger et al., 2009; Mohajeri et al., 2016). From a micro perspective, the spatiotemporal characteristics of solar radiation within an urban canyon strongly depend on sky obstruction by adjacent buildings and tree canopies (Gong et al., 2018). Global solar radiation inside high and low rise canyons can create asymmetry patterns and vary up to three times in summer and five times in winter (Gong et al., 2019). Such irregularities of solar radiation are inevitable in complex canyons (Jamei and Rajagopalan, 2017). The asymmetry pattern of solar radiation inside the buildings can also lead to local thermal discomfort (Marino et al., 2017). Therefore, rendering solar radiation within the urban canyons is vital to understand better the interactions between solar radiation and human health (Gong et al., 2019). Moreover, ignoring irregularities in solar radiation can significantly misrepresent visual comfort by creating a sudden leap from an intolerable to an imperceptible status (Balakrishnan and Jakubiec, 2016). Given the importance of solar radiation's incidence within and around buildings, assessing urban geometry can help draft guidelines for different stakeholders (Strømann-Andersen and Sattrup, 2011). Therefore, an interdisciplinary attitude is required to holistically evaluate occupants' sensitivity to the built environment (Andersen, 2015).

1.2 The nature of uncertainties in urban canyons

Based on the available knowledge about each uncertain parameter, two natures of uncertainty are defined, i.e., epistemic and aleatory. The aleatory nature of uncertainty is stemmed from the inherent randomness of parameters that can be well-defined by distributions. Epistemic uncertainty, on the other hand, is attributed to the lack of knowledge (Kiureghian and Ditlevsen, 2009). Studies have recommended probabilistic treatment of aleatory uncertainty, i.e. using probability distribution functions. However, for epistemic uncertainty, it is suggested to opt for a possibilistic representation, namely, using possibility distribution functions (Dubois and Prade, 2001). A mixture of both aleatory and epistemic uncertainties is observed in urban canyons (Mao et al., 2017). For instance, the uncertainty associated with adjacent buildings' height can be handled through the probability theory, as numerous in-situ measurements of this parameter can yield a well-fitted probability distribution. On the other hand, for some parameters such as the transmittance of trees, the possibilistic treatment is preferable due to insufficient data on its variation. Hybrid probabilistic-possibilistic treatment of uncertainty is recommended for analysing

uncertainties within a complex model, as it excels in handling heterogeneous levels of information (Guyonnet et al., 2003). This challenge can be extended to the context of urban microclimate, which contains both aleatory and epistemic natures of uncertainty.

1.3 Research objectives and original contribution

As discussed, there is a strong dependency between the behaviour of solar radiation within urban environments and the characteristics of the urban canyon. Therefore, there is a need for a scheme that captures uncertainties associated with solar radiation within canyons, adequately propagates them according on their nature, and eventually quantifies their effects on indoor environment. The objective of this study is to address this challenge by presenting a novel framework and demonstrate its practicality through a case study.

First, the study is focused on complex canyons. Here, the term complex implies that (1) the skyline of the canyon is not a straight line, (2) the external reflectances of adjacent buildings differ from one to the other, (3) the glazed area is not a fixed value along the canyon length, (4) the trees are modelled with two uncertain features, i.e., size and transmittance, and (5) parked cars are also considered as components of a complex urban canyon.

Second, the idea of considering a purely probabilistic treatment of uncertainty is challenged by stressing that heterogeneous levels of information are associated with different parameters. Instead, a hybrid probabilistic-possibilistic approach is suggested as a solution to handle various levels of information.

Third, the impacts of uncertainties in the urban canyon are evaluated separately on thermal and visual comforts. These assessments are followed by a discussion on simultaneous thermo-visual comfort. Given the co-variance of thermal and visual comfort, a new visualization technique is proposed for comparing the results and supporting the decision process.

This study shows how rescaling the building boundary conditions from mesoscale to microscale can provide further insights into the building performance assessment, and that the initial requirements (i.e., informative priors) should be locally measured. Moreover, a meta-heuristic attitude ought to be taken towards the inputs of building performance estimation tools. The framework here introduced can help the development of the next generation of models supporting decision-makers, including architects, building engineers, and urban planners.

2. Methods

2.1 Uncertainty treatment and uncertain parameters

The application of hybrid uncertainty treatment in building performance simulations has been previously discussed (Khayatian et al., 2018). This study opts for a similar approach to treat the uncertainties within urban canyons. For the sake of brevity, details about the adopting framework in (Khayatian et al., 2018) for hybrid approach and possibilistic distribution on epistemic parameters are offered in Appendix A.

Seven input variables are selected as uncertain parameters in urban canyons. Table 1 reports each variable's characteristics, including units, range of variation, and nature of embedded uncertainty. The term "survey" in Table 1 refers to authors' observations from actual urban canyons located in Milan, Italy. Using Google street view images, the characteristics of six typical urban canyons with similar aspect ratios and different vegetation covers (no tree, small trees, large trees) are analysed. Images are then scaled based on a typical height of 3.2 m per floor. Buildings' height, glazed area (WWR), and the reflectance of opaque surfaces are extracted from the scaled images. The survey shows that the height of the surrounding buildings fluctuates by ±10 % from the average building height, while the WWR varies between 15 % to 60 %. Based on the façade colours and materials, the reflectance of surrounding buildings ranges between 0.1 and 0.3. Given that the survey could not provide reliable information on tree transmittance and car reflectance, the uncertainty associated with these values is assumed to have an epistemic nature and therefore represented through the theory of possibility. The transmittance of trees and the reflectance of car bodies are derived from measurements obtained from (de Abreu-Harbich et al., 2015) and (Levinson et al., 2011). All solar radiation analyses within the urban canyon performed in DIVA 4 (Grasshopper plug-in) (Solemma, 2014), an optimized and climate-based simulator of daylight and energy of different scales from a single building to the urban scale.

Table 1- uncertain parameters in urban canyon and range of variation.

	Uncertain parameters	Unit	Variation	Definition of uncertainty
1	Ratio of building height	%	±10 % (survey)	Probabilistic
2	WWR	%	[15 , 60] (survey)	Probabilistic
3	External shading	On/off	[0 , 1] (scenario)	Probabilistic
4	Exterior wall reflectance	-	[0.1 , 0.3] (survey)	Probabilistic
5	Trees crown dimeter	m	[4.5 , 10] (Perini and Magliocco, 2014)	Probabilistic
6	Tree transmittance	-	[0.2 , 0.3] (de Abreu-Harbich et al., 2015)	Possibilistic
7	Cars reflectance	-	[0.05 , 0.58] (Levinson et al., 2011)	Possibilistic

2.2 Investigation on modelling trees in the urban canyon

The transparency of trees is modelled by resorting to the translucent sphere object, which has been verified as an acceptable solution (Balakrishnan and Jakubiec, 2016)(Tregenza and Wilson, 2013). A translucent object is defined by the Trans type of material in the RADIANCE material database (Crone, 1992). However, a detailed investigation of several tree models is executed to justify the simplified model. Consequently, two common approaches in tree modelling are compared: (1) a simple sphere with reflected winter/summer change in material properties attained by assigning different transmittance values, and (2) a detailed geometry where the seasonal change is shaped by randomly changing the leaf area percentage. Then, two black boxes with an open cap and a grid of irradiation sensor (facing up) on the floor are covered with two symbolic geometries (Figure 1). In Figure 2, the green boxplots refer to the simple geometry, where the winter and summer

transparency of trees to solar radiation is defined as 0.82 and 0.41, respectively. In the detailed models, the leaf area percentage is randomized to simulate trees' winter and summer shape. The comparison results revealed that Rand4 could suitably present winter transparency, while Rand2 can be considered a summer tree (Figure 2). However, such detailed modelling of trees significantly increases the computational time, which is double for highly dense single tree (Rand2) was twice longer than that of a simple tree model. This extra computational time is utterly crucial for this study. Therefore, the uncertainty analysis of the urban canyon in this study is developed based on a simple tree geometry, while seasonal effects are reflected within the material.

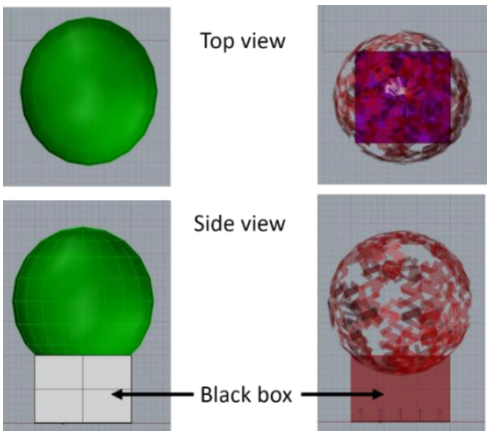

Figure 1- The model in which transmittance of trees evaluated in a simple sphere with Trans material versus detailed tree with randomness on leaf.

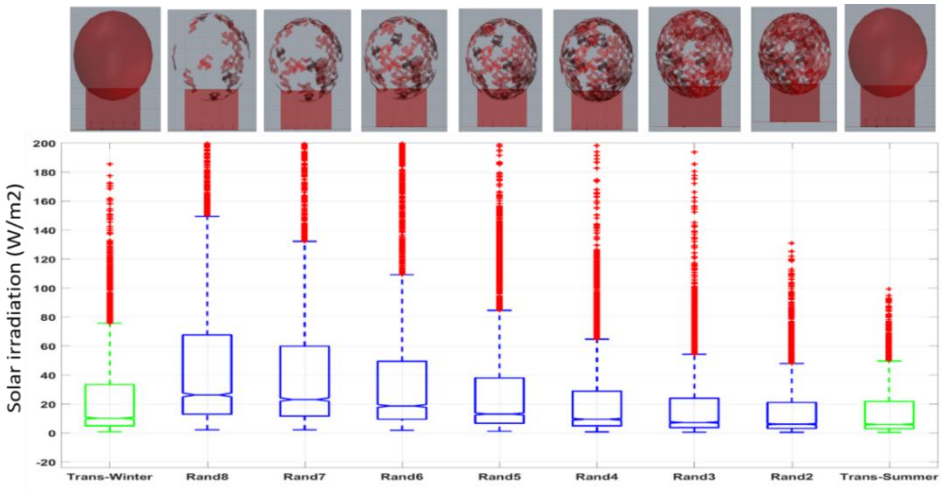

Figure 2- Sensitivity analysis of detailed tree vs. simple sphere, the decision about a precise model, or relying on Trans material. Rand1 to Rand8 model various tree transmittance by randomness in leaf area percentage.

2.3 Model description

All simulations of this study are performed in the context of Milan, Italy (45.46° N, 9.19° E). The measured weather parameters used for the simulations include air temperature, relative humidity, global horizontal radiation and diffuse horizontal radiation, collected during 2016. The global solar radiation is measured with a Kipp Zonen CMP 22 secondary standard pyranometer and the diffuse

radiation with a CMP 21 under a shadow band, while the other parameters are measured by a Vaisala WXT 520, with all sensors being at Politecnico di Milano (details in (Curci et al., 2017)). All sensors are regularly maintained and managed according to ISO 9001, with the calibration of the thermohygrometer performed in a climatic chamber (Curci et al., 2017).

The framework of uncertainty quantification of a complex urban canyon is developed on a sample case study. The case study is a canyon with an aspect ratio of 0.5 and E-W street orientation. All simulations, including radiation map, thermal, and visual comforts, are performed with two groups of scenarios: (1) A simple canyon scenario (Figure 3-b), and (2) uncertainty associated scenarios composed of 60 random samples generated by a hybrid approach (Figure 3-d). The possibilistic parameters in Table 1 require a minimum of three α-cuts for proper representation (see Appendix A). Therefore, the possibilistic distributions return six values corresponding to all plausible events. The hybrid uncertainty propagation framework requires every random value to be associated with each of the plausible events. To balance the simulation time and the accuracy, we used the minimum number of random samples (10), that when combined with all plausible events (6), return a total of 60 hybrid scenarios. Although the minimum number of random samples and α-cuts are utilized in this study, they are adequate to highlight the effect of uncertainties on indoor visual and thermal comfort. However, it should be noted that increasing the number of (or regenerating different) random samples has dissimilar effects based on the model's response to different parameters. For instance, the "ratio of building height" (Table 1) randomly assigns a value to each building's height. The variation of this parameter creates different shapes of canyon skylines and has a non-monotonic effect on the incident solar radiation. Therefore, increasing the number of samples (or regenerating different samples) related to the "ratio of building height" could produce additional uncertain scenarios not covered in this case study. On the other hand, the model's response to other uncertain parameters such as "WWR" and "Exterior wall reflectance" (Table 1) is monotonic. For these variables, increasing the number of samples would not affect the range of variation in the outputs but increase the resolution of the output range.

The inclusion of a deterministic scenario and uncertainty analysis can help decision-makers better understand the design choices (Chen et al., 2017). The exterior surfaces of top, middle, and ground floors are studied for quantifying incident solar radiation. However, for brevity, detailed thermal and visual comfort analyses are only evaluated for the middle floor and only the effect of uncertainty on south façades is discussed.

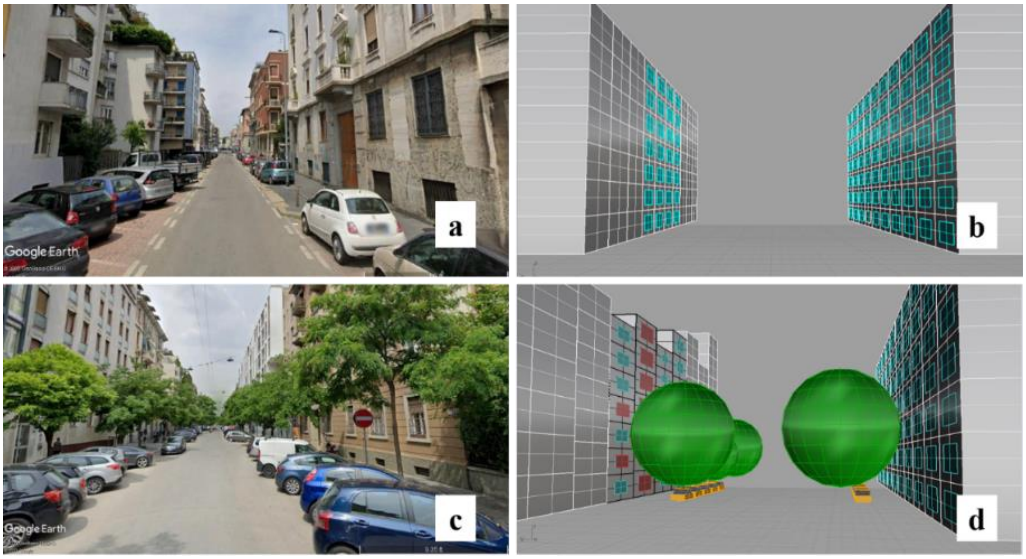

Figure 3 – Samples of actual canyon layouts in contrast with modelled versions. No tree-real canyon (a), With tree-real canyon (b) Simple canyon model (c) and a sample of complex canyon model (d).

2.4 Thermal comfort with solar-based PMV

For indoor thermal sensation, the Predicted Mean Vote (PMV) is perhaps the most commonly used approach (Fanger and others, 1970), which still ignores the effect of shortwave solar radiation on thermal sensation, despite its notable impact on human thermal comfort. La Gennusa et al. (La Gennusa et al., 2007) and Arens et al. (Arens et al., 2015) presented different methods to include solar radiation's effects on the MRT. This study follows the method by Arens et al. (Arens et al., 2015) to involve shortwave radiation on MRT (MRT_{solar}) while including the impact of uncertainties in building boundary conditions. The MRT_{solar} is then used to calculate the indoor PMV. Here, we opt for extended PMV for non-air-conditioned buildings (Ole Fanger and Toftum, 2002). The inclusion of solar radiation in thermal comfort is denoted as "*solar-based PMV*".

The required variables to perform solar-based PMV calculation is reported in Table 2. The Hourly-simulated and Hourly-calculated variables in Table 2 are climate-based variables that should be individually estimated for each climate condition. Therefore, global, direct, and diffuse components of incident solar radiation (I_{global}, I_{diff}, I_{dir}) are retrieved from the uncertainty analysis of the studied urban canyons from DIVA simulations. Also, the hourly values of the projected area factor (f_p) for seated posture are derived from a fitted curve on the reported sun azimuth/altitude and projected area factor (Kubaha et al., 2004). The mentioned fit is an interpolation by MATLAB curve fitting tool (The MathWorks, 2018) to form a polynomial function. The hourly values of f_p are extracted from fit function, as reported in Eq.1.

$$f_p(h) = FittedModel(SunAzimuth_h, SunAltitude_h). \quad \text{(Eq.1)}$$

Table 2- Input parameters for calculating MRT solar, Units and used values in the following calculations.

Input parameters	Unit	Value
f_{eff}	-	0.755
f_{svv}	-	0.28
I_{diff}	W/m^2	Hourly-simulated
I_{global}	W/m^2	Hourly-simulated
I_{dir}	W/m^2	Hourly-simulated
R_{floor}	-	0.2
A_p	m^2	Hourly-calculated
f_{bes}	-	0.3
A_D	m^2	1.8
T_{sol}	-	0.71
$\propto_{Sw}$	-	0.67
$\propto_{Lw}$	-	0.67
f_p	-	Hourly-calculated
Window Width	m	1
Window Height	m	1.6
Occupant distance to the window	m	0.5

Finally, the hourly values of f_p are utilized to calculate exposure to direct beam radiation (A_p). These quantities are fed into Arens et al. (Arens et al., 2015) equations to calculate the ERF_{solar} (Effective Radiant Field) and estimate the MRT_{solar}, with the inputs offered in Table 2.

The indoor environment calculations, including temperature and relative humidity, are performed by WUFI Plus (V. 3.1.1.0) (Holm et al., 2003), a whole building simulation tool that computes the heat and moisture balance and transport through building components (Antretter and Winkler, 2015). WUFI accepts measured solar radiation over a particular inclination as input for simulation (Fraunhofer-Gesellschaft, 2019). Therefore, to incorporate the estimated radiation from a complex canyon in building simulations, the hourly incident solar radiation on the south façade is extracted from DIVA outputs and insert into the WAC weather data.

The simulated zone is a chamber in the middle floor of a seven-story building, with a size of 10 m × 5 m × 3 m and a 60 % ratio of WWR. Other floors are considered to have adiabatic partitions between conditioned space. The building model is conditioned during the heating period (winter). Building characteristics, including building components assembly, infiltration rate, and system characteristics, are chosen based on typical buildings for Milan (Paolini et al., 2017). The studied building model is placed in the middle of the urban canyons. Since the effect of ground reflectance and surrounding elements is already taken into account by DIVA calculations, these are excluded from the WUFI model. Indoor temperature and relative humidity are extracted from all simulations as sources of solar-based PMV calculations.

The thermal sensation based on the Chartered Institution of Building Services Engineers (CIBSE) (Humphreys and Nicol, 2015) is categorized into 7-points scales, including (hot, warm, slightly warm, neutral, slightly cool, cool, cold). Some studies proposed finer scales of PMV, including:

with 9-points (Salata et al., 2016) and 13-points (Buratti et al., 2016). The predicted percentage of dissatisfied people metric (PPD) is often used alongside PMV and reports the percentage of people dissatisfied with thermal comfort. The limiting criteria for comfort, according to ASHRAE's recommendation, is PMV ±0.5 and PPD 10 % (Standard, 2010). Mapping the comfort definition by ASHARE (Standard, 2010) on the 13-points scale of PMV (Buratti et al., 2016), this study considers a collective approach. Accordingly, finer scales, including "Between Neutral and Slightly Cool" (BNSC), "Neutral" and "Between Neutral and Slightly Warm (BNSW)" (see (Buratti et al., 2016)).

2.5 Visual comfort with DGP

Among the different metrics for evaluating visual comfort, Daylight Glare Probability (DGP) is suggested as a robust metric to estimate the daylight glare during the design (Wienold and Christoffersen, 2006) (Iwata et al., 2017). Glare sensations in the DGP metric can be classified into four scales (Jakubiec and Reinhart, 2012): "Imperceptible" (DGP < 0.35), "Perceptible" (0.35 ≤ DGP < 0.4), "Disturbing" (0.4 ≤ DGP < 0.45), and "Intolerable" (0.45 ≤ DGP). Therefore, a similar approach is adopted for visual comfort analysis in this study. Accordingly, a daylight camera is located in the middle of the chamber, with 2 m distance from the window, in the human eye-level (h = 1.2 m), directly facing the window (Figure 4). The typical office schedule of 8-18 is considered for daylight analysis. However, the hours during which the sun is under the horizon are excluded from the calculations. Therefore, in March and June, calculations are performed between 9 am to 6 pm, while in December, only 9 am to 3 pm is simulated. The glare calculations are performed in DIVA-4 and under clear sky conditions. Figure 5 shows the framework of simultaneous thermal and visual comfort evaluations under uncertainties in any urban canyon by adopting the hybrid probabilistic-possibilistic approach.

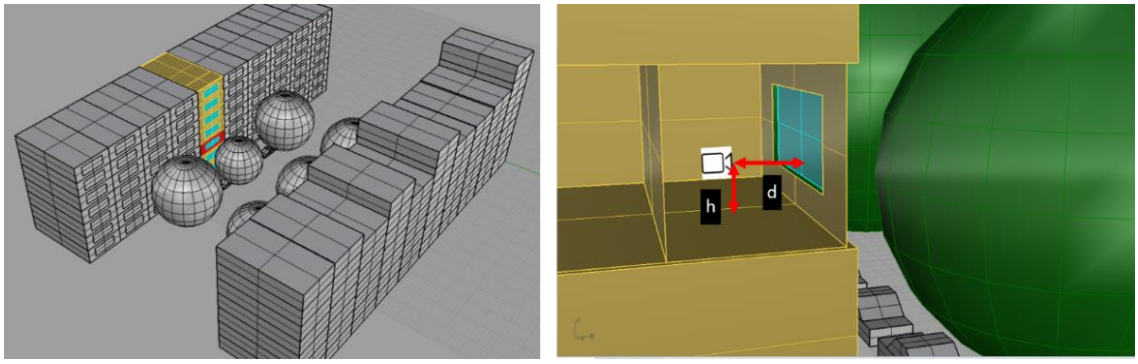

Figure 4- Left: Outside view of studied glare area (highlighted by red colour), a sample of the complex urban canyon- Right: Inside view of posed daylight camera on the middle floor where h=1.2 m, *d=2* m.

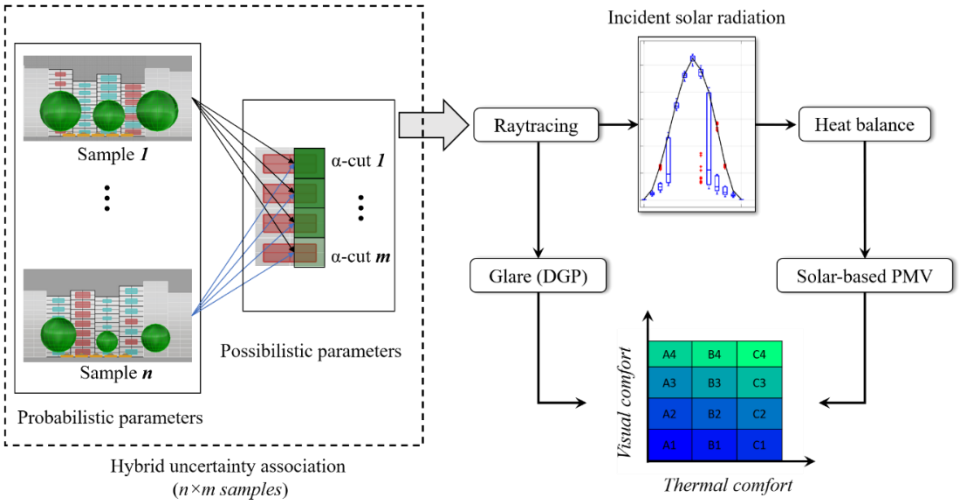

Figure 5 - A framework for the hybrid treatment of uncertainties within an urban canyon and quantifying the effects of uncertainty in solar radiation on visual and thermal comfort.

3. Results and discussion

The first series of simulations (i.e., estimations of incident solar radiation) is performed for all 60 randomly generated samples. Post-processing the DGP results revealed that the first α-cut (transmittance of 0 and 1 for trees, see Appendix A) did not follow a logical trend. Therefore, in DGP and solar-based PMV simulations, all samples within the first α-cut are excluded from the analysis, which reduced the total number of evaluated samples to 40.

3.1 Solar radiation in the complex canyon

Incident solar radiation in hourly time steps is simulated over the south façade and for the highlighted area in Figure 4-left. Then, the simple canyon scenario contrasts with uncertain scenarios through the daily profiles of typical solar days (Figure 6). Accordingly, three days are highlighted as the typical solar days for summer, midseason, and winter, selected to represent the highest, intermediate, and lowest solar elevation during a clear sky condition. Therefore, the daily profiles for 21st March, 20th June, and 22nd December are the chosen as representative days (measured 21st June and 21st December did not offer clear sky conditions). The first observation points to the difference between the probabilistic approach and the deterministic approach of modelling the boundary conditions (Figure 6). For the deterministic approach (simple canyon), a single value is obtained for each hour. However, the probabilistic approach (random complex canyons) provides a range of variation for each hour of the day within which the actual incident radiation exists. A comparison between deterministic and uncertain scenarios shows how the single scenario can over/underestimate incident solar radiation (Figure 6).

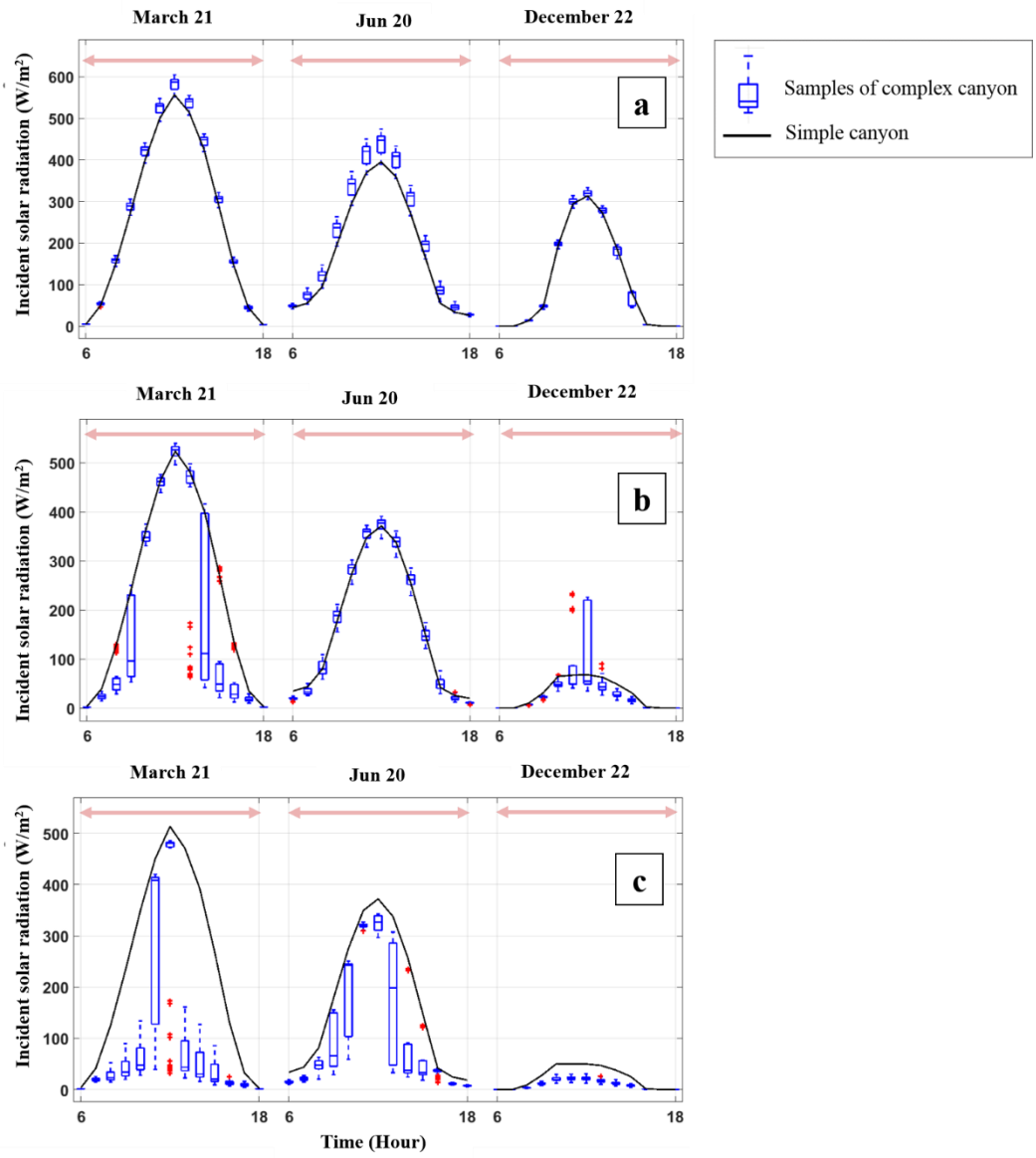

*Figure 6 - Simple canyon vs. uncertainty propagated canyon - Daily profile of solar radiation in three levels of the building (**a**: top floor, **b**: middle floor, and **c**: ground floor) 21st March, 20th Jun, and 22nd December.*

In a multi-layer urban canopy, complexities along with its height project different impacts on intercepting or exerting solar radiation (Krayenhoff et al., 2020). Similar effects are reproduced by generating random canyons (Figure 6):

- Building surfaces of top floors are less sensitive to urban canyon uncertainties (Figure 6-a) and mostly receive unobstructed solar radiation, with slight variations due to the skyline of the canyon (the first parameter in Table 1).

- The variation of solar radiation on the middle floor is jointly due to the canyon skyline and the trees. These effects are visible on the middle floor during the intermediate and winter seasons (Figure 6-b), while in summer the variation is lower due to the high solar position angles and shorter shadows.

Different patterns of incident solar radiation are observed on the ground floor. This area mostly receives diffuse solar radiation since the skylines constantly cast shadows on the ground floor, while the trees block diffuse radiation.

3.2 Urban canyon and indoor thermal comfort

Based on the presented framework (Figure 5), the results of the uncertainty quantification of incident solar radiation are delivered to building simulation models in WUFI. Indoor temperature and relative humidity are retrieved from WUFI simulations, and then, MRT_{solar} is calculated as highlighted in section 2.3. Alongside MRT_{solar}, metabolic rate (1.2), clothing rate (define based on hourly outdoor temperature) and air movement (0.1 m/s) are the inputs of traditional PMV calculations. The results of solar-based PMV (Figure 7) reveal a pattern of variation similar to the incident solar radiation on the middle floor (Figure 6-b). The most significant variation of solar-based PMV occurs during the midseason, while slight discomfort is computed during winter, due to overheating from exposure to direct radiation, which is underestimated with a simple canyon.

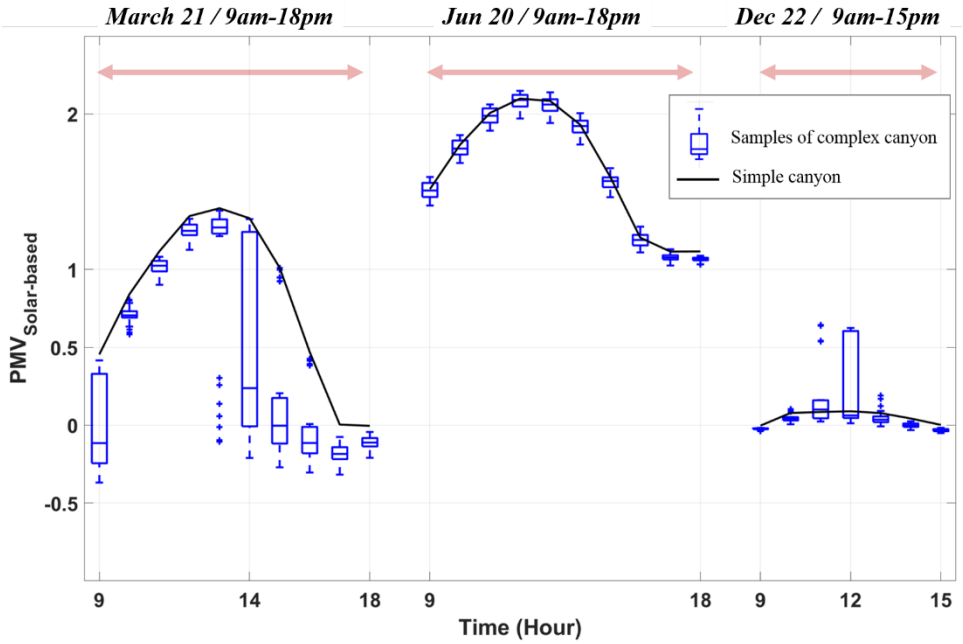

Figure 7- Simple canyon versus uncertainty propagated canyons, solar-based PMV for typical solar days of intermediate, warm, and cold seasons (left to right).

Figure 8 demonstrates how solar radiation's uncertain behaviour can shift the different comfort bins within the canyon. The daytime hours are classified for one year of hourly simulations in PMV scales (see section 2.3). The difference between the deterministic and hybrid approaches is mainly visible as a misrepresentation of the "Neutral" sensation. The simple canyon underestimates the "Neutral" occurrences by 70 hours at best, and 365 hours at worst case. It is also interesting to assess the density of hours in "BNSW" as this scale represents the upper threshold of thermal comfort. Ignoring the uncertainties in an urban canyon could overrepresents "BNSW" occurrences in a year by 146 hours. The moderate scales (i.e., "slightly warm" and "warm") show less sensitivity to uncertainties in outdoor boundary conditions. However, the trace of uncertainty in the canyon elements during the "hot" hours is visible, as a simple canyon could overestimate the "hot" hours by 218.

The impact of hybrid treatment of uncertain features is illustrated in Figure 9 by evaluating uncomfortable hours, and contrasting the probabilistic treatment of uncertainty against a possibilistic approach by comparing the number of uncomfortable hours. The limiting criteria for the comfortable scale, as noted, follow ASHRAE's recommendation of PMV of ±0.5 (Standard, 2010). Black lines (dash & solid) show the effect of the seasonal change in trees transmittance, represented by a possibilistic approach. The red lines (dash & solid) report the effect of aleatory uncertainty, represented by probabilistic variables (Table1). Figure 9 underlines the shadowing effect of trees within a complex canyon and the consequent effects on building performance. The difference between the lower bounds (black dash) and upper bounds (black solid) of possibilistic variables is 257 hours during a year, which is 18 times more than the probabilistic variables.

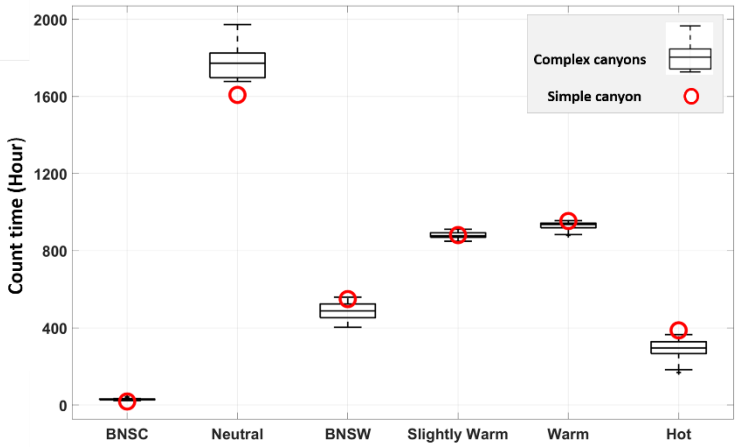

Figure 8- Mapping thermal sensation with solar-based PMV; A comparison between simple scenario and uncertainty associated scenarios.

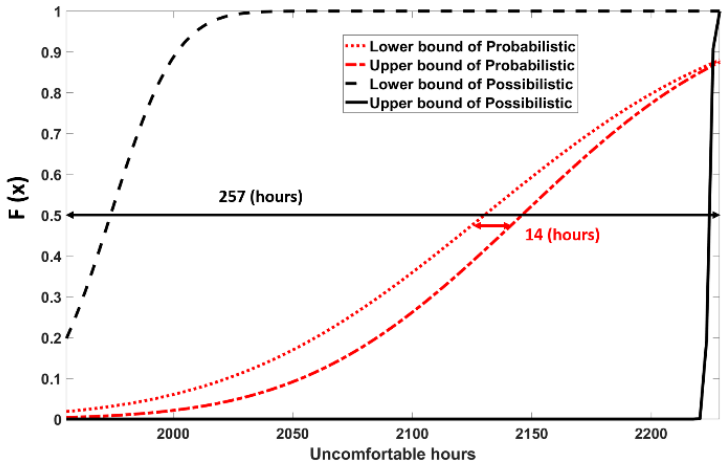

Figure 9- Contrasting the effect of probabilistic and possibilistic variables on uncomfortable hours based on ASHRAE-55 threshold (PMV ±0.5).

3.3 Urban canyon and indoor visual comfort

Results of DGP are extracted from the glare simulations in DIVA (Figure 10), including a comparison with a simple scenario. Similar to solar-based PMV results, the probability of the glare also follows the pattern of solar angles. Accordingly, smaller variations in the summertime and

higher sensitivity during the midseason and wintertime are the main effects of uncertainty on DGP. The glare sensation within a canyon during the summertime is mostly within the "imperceptible" (DGP < 0.35) and "perceptible" ($0.35 \leq$ DGP < 0.4) scales. However, during midseason, the estimations of DGP within a simple canyon are mostly at 1.0 ("intolerable"), while the uncertainties can drop the DGP as low as 0.28 ("imperceptible") throughout the day.

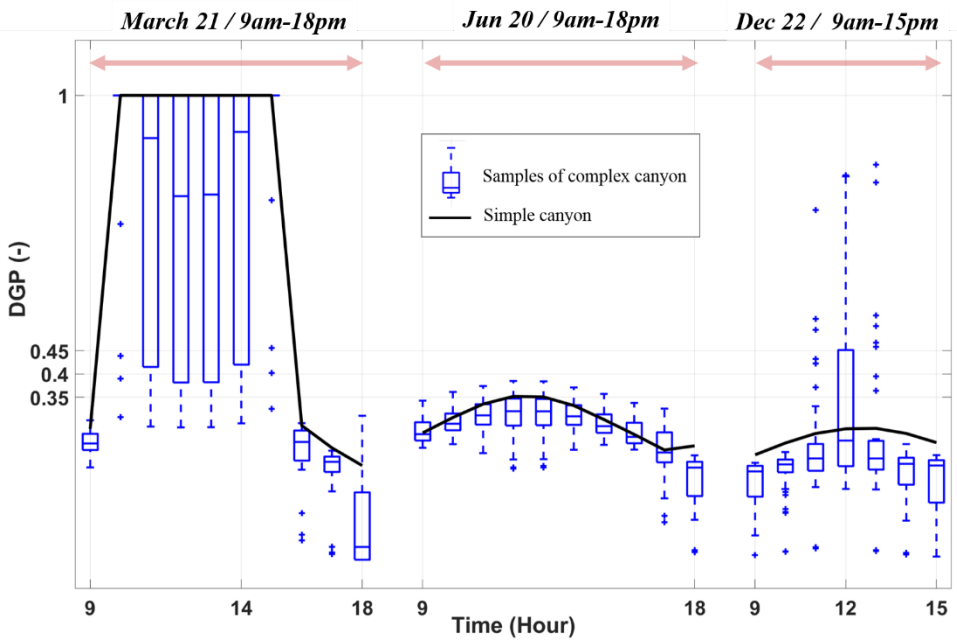

Figure 10- Simple canyon versus uncertainty associated canyons, DGP for typical solar days of intermediate, warm, and cold seasons (left to right).

3.4 Thermo-visual comfort analysis

In this section, we present a set of combinations to evaluate both visual and thermal comforts simultaneously, with two main objectives: (1) to quantify how comfort could vary in uncertain urban canyons according to conventional metrics, and (2) to highlight where the proposed analyses can be useful for decision support.

For the first objective, a Sankey diagram (Figure 11) demonstrates the balance of thermal and visual comfort within the studied periods, and facilitates a comparison of simple and uncertain scenarios and visual and thermal comfort. Four sets of information are reported in Figure 11. The left side of Figure 11 focuses on thermal comfort, stressing that the uncertainties in the urban canyon during summertime would have low effects on the "warm" scale of solar-based PMV. Therefore, in peak summer, uncertainties associated with size and transmittance of trees have a trivial effect on solar-based PMV. Figure 11 also shows that opting for a simple canyon scenario may underestimate thermal comfort hours. For instance, the percentage of "neutral" hours in one of the random scenarios reaches as high as 52 %, which is roughly 10 % more than the simple scenario.

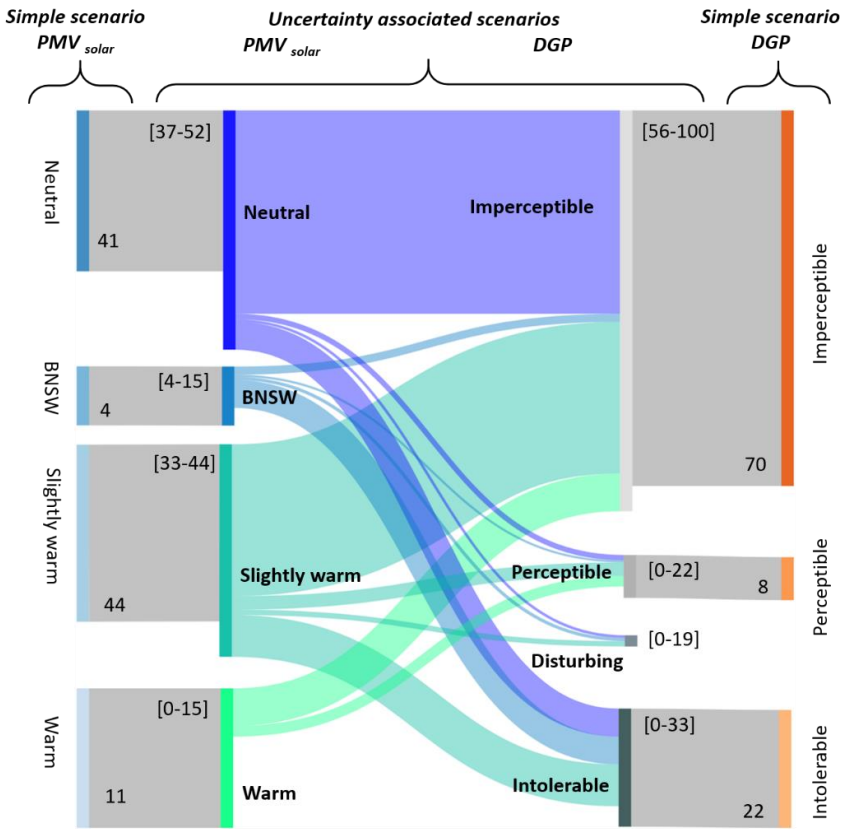

Figure 11 – Sankey diagram of thermal comfort distribution to visual comfort scales; Single numbers are the percentage of hours for each scale of comfort in simple scenarios. The ranges are related to complex canyons.

The right side of Figure 11 focuses on visual comfort, where a simple canyon is contrasted against random scenarios. It is observed that the effects of uncertainty are noticeable in all categories of the DGP measure. For instance, the percentage of hours falling in the "imperceptible" class of DGP has a wide range of variations, ranging between 56 % to 100 % hours in random samples. Meanwhile, the simple scenario shares about 70 % of the hours in the "imperceptible" class, close to the median of random scenarios. Therefore, a simple canyon scenario may return similar glare performances to a complex one. With such a high range of uncertainty, the designer is prone to overlook the number of uncomfortable hours.

Focusing on the central section of Figure 11 reveals two crucial facets. First, some portions of the thermally "neutral" scale are connected to visually "intolerable" glare conditions. This is due to the low solar angles during winter. In such conditions, thermal comfort and visual discomfort are observed simultaneously. Therefore, improving visual comfort without heavily affecting thermal sensation requires an in-depth analysis. Second, the "slightly warm" thermal sensation is mostly split between "imperceptible" and "intolerable" levels of glare. These facets call for a detailed analysis of the shading control strategy. If an actuator is solely activated based on visual comfort criteria, the corresponding impacts on thermal comfort should not be overlooked. The proposed holistic approach can be a basis for multicriteria automated shading systems, which has been previously implemented through a fuzzy controller in (Kristl et al., 2008).

For the second objective, we explore the random samples that display the most significant variation in both solar-based PMV and DGP. As a result, 21st March at 2 pm is selected for further assessment. The colours in Table 3 refer to the multisensory comfort sensation. Each direction in Table 3 provides a specific set of information. Columns present a view of the probabilistic parameters, while rows offer a view of the possible parameters (Figure 13). Since this part of the study is focused on the middle floor, the effects of car reflectance are minimal, and therefore, the possibilistic uncertainty is dominated by tree transmittance. Figure 12 provides a legend for the colours in Table 3. Each class of Figure 12 (from A1 to C4) represents a joint thermal and visual comfort class. For example, A1 refers to instances in which glare is "imperceptible," and PMV is in the "neutral" scale. Figure 15 in Appendix B provides a set of false-colour images from all simulated samples and hours.

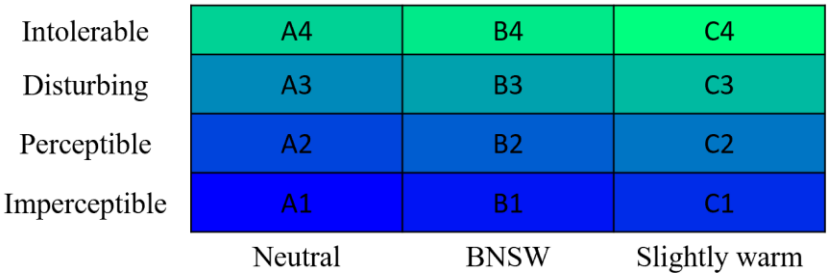

*Figure 12- Legend to read Table 3, **Horizontal** axis shows the observed scales of solar-based PMV; the **Vertical** axis refers to the classes of DGP.*

From Table 3, through the geometries with larger trees (e.g., G_1^j) the changes of DGP from "imperceptible" to "intolerable" correspond to the changes in transparency from 0.1 to 0.7. In the samples with smaller trees, the impact of transparency is less evident, given that trees do not obstruct solar radiation (G_2^j and G_4^j). In these samples, "intolerable" DGP occurs with a "slightly warm" sensation. Impacts of the height of surrounding buildings are visible in G_8^j and G_9^j, with concave skylines. Given the concave skyline, and despite the large tree size, "intolerable" DGP is observed along with "slightly warm" thermal sensations.

Table 3- A sample pattern to provide support information for design; The pattern shows the simultaneous of visual and thermal comforts in candidate hour in all random samples; G_i^j returns the random canyon in which j and i refer to the probabilistic and possibilistic iterations in Figure 13.

		G_1^j	G_2^j	G_3^j	G_4^j	G_5^j	G_6^j	G_7^j	G_8^j	G_9^j	G_{10}^j
March-21	$\underline{G_i^2}$ (Trans 0.1)	A1	C4	A1	C4	A1	A1	A1	C4	C4	A4
(2 pm)	$\overline{G_i^3}$ (Trans 0.2)	A2	C4	A2	C4	A2	A2	A2	C4	C4	A4
	$\underline{G_i^3}$ (Trans 0.3)	A3	C4	A4	C4	A4	A3	A4	C4	C4	A4
	$\overline{G_i^2}$ (Trans 0.7)	A4	C4	A4	C4	A4	A4	A4	C4	C4	A4

3.5 Discussion

Incident solar radiation greatly influences indoor thermal and visual comfort (Marino et al., 2017) (Balakrishnan and Jakubiec, 2016). On the other hand, solar radiation is affected by the complexities within an urban canyon (Gong et al., 2019)(Krayenhoff et al., 2020). This study proposed a framework for modelling and assessing uncertainties associated with solar radiation in urban canyons (Figure 5) to evaluate how solar radiation affects indoor visual and thermal comfort within the urban context.

A proper representation of uncertainty based on the nature and availability of data is key to obtaining a realistic perception from the environment (Khayatian et al., 2018). This study resorts to the possibilistic representation of the uncertain parameter "tree transmittance", as little to no information was available from the literature (Table 1). This approach results in high fluctuations of incident solar radiation during midseason in the middle and ground floors, as they are most affected by tree transmittance (Figure 6). These findings are aligned with observations of another field study, in which the highest fluctuation of shading coefficients was observed during the midseason (Berry et al., 2013).

Previous studies reported the highest variations in the MRT_{solar} when the solar angle is low (Zomorodian and Tahsildoost, 2017). These field measurements support our findings that solar-based PMV is extremely sensitive at lower solar angles (Figure 7). This behaviour of solar-based PMV is also in agreement with observations from (La Gennusa et al., 2007), with comparable solar angles and solar intensities.

The representation approach for thermo-visual comfort (Table 3) follows recommendations by (Ko et al., 2018), who argue that an integrated representation approach can facilitate decision-making in complex environments with a multitude of variables. However, here we tried to take the integrated visualization approach a step further by highlighting the co-occurrence between thermal and visual discomfort (Figure 11). Furthermore, representing deterministic results along with uncertainty analysis has proven to facilitate the decision-making process. (Chen et al., 2017). This study has adopted a similar attitude by complementing uncertainty analyses with deterministic scenarios (simple scenarios) as supportive information for a wide audience range.

Here, the random input parameters are assumed to have no covariation, and therefore, are represented by separate probability distribution functions. However, this assumption could potentially overrepresent rare events and result in overestimating the effects of uncertainty. Condition to availability of adequate data, Gaussian mixture models can be formed to account for co-dependencies between uncertain inputs. Furthermore, this would allow to fit a surrogate model onto the inputs and outputs and overcome the computational burden by directly sampling from the surrogate model (Vu-Bac et al., 2016). This approach is particularly useful for replacing heavy computations such as the solar radiation calculations utilized in this study. Accelerating the calculation process is not only limited to Gaussian mixture models, as recent advances in deep learning can return fairly accurate predictions of highly complex models. In this study, calculation outputs of solar radiation from on simulation engine (DIVA) were fed to a second simulation model (WUFI) to estimate indoor thermal comfort. This entire process can be facilitated through physics-inform deep neural networks and save computational time (Samaniego et al., 2020).

3.6 Limitation and future development

The proposed uncertainty quantification method of solar radiation is only tested for the south façade as a case study representing the most critical surface in the northern hemisphere. Other orientations have not been included in this study for brevity; however, applying the proposed method on various inclinations and orientations is highly recommended. This issue may be more challenging for daylight analysis for east and west orientations. This study presented solar radiation estimations in urban canyons regarding the effects of uncertain parameters, and the effects on occupant comfort are clarified. Our findings can be further extended to decision-making tasks at the design phase, such as relatability assessments of different shading systems.

Further, the thresholds of DGP scales are the subject of ongoing research, given that the cut-off values may differ between lab experiments and field studies (Pierson et al., 2019). Here, we proposed a fuzzy approach for representing uncertainties associated with building surroundings but did not consider the imprecision of the crisp DGP thresholds. Considering the fuzzy nature of the sensation of comfort, other classification methods such as the Fuzzy Analytic Hierarchy process can complement the method introduced in this study. The application of this process has been previously demonstrated for evaluating building performance (Hu et al., 2019).

4. Conclusions

The conventional approaches to modelling urban canyons were challenged and compared with more complex and detailed representations. The complex canyon model is evaluated for its impacts on incident solar radiation on building surfaces. Thermal and visual comforts are studied in detail, and the effects of uncertainties are contrasted against both comfort metrics simultaneously. Previous studies mainly focused on outdoor thermal comfort affected by the canyon and solar availability in micro-urban scales or glare analysis in a case-specific condition. From the evaluations on the case study, the following outcomes are observed:

a) Different sources of uncertainty in an urban canyon justify the application of a hybrid approach to represent and propagate the uncertainties. Further analysis of indoor solar-based PMV showed that the effect of variables with high uncertainty (treated according to the theory of possibility) could be considerably greater than features with lower levels of uncertainty (treated based on the theory of probability).

b) A comparison between simple and uncertainty associated (complex) canyons revealed the significant risk of over/underestimating comfort conditions when resorting to the conventional and simplified modelling of a canyon. A simultaneous assessment of thermal and visual comfort showed that they do not necessarily co-vary, and therefore, an in-depth joint evaluation of both metrics is inevitable.

c) The parameters that affect the solar radiation indoors can greatly vary based on different characteristics, and therefore, a *fit for all* assumptions is not recommended even for buildings within the same canyon. As an example, for the middle level of a typical canyon, apart from the

solar angle, the (1) size of the tree, (2) transmittance of the tree, and (3) skyline of the canyon can impact thermal and visual comfort.

d) It was observed that details of the urban canyon, such as variation in adjacent buildings' height and transparency of surroundings, could drastically affect thermal and visual comfort. These effects vary in seasons based on the sun position; for instance, less sensitivity to outdoor uncertainty is observed during the summer. The sensitivity of comfort metrics to microclimate uncertainty is mainly observed during the cold and intermediated seasons if no cooling system is installed. It was also shown that the effects of uncertainty are sensitive to the room's elevation and vary on different floors.

Therefore, the consideration or not of uncertainty can lead to different design decisions, including the evaluation of the need of different degrees of adaptability of the façade to the environmental stimuli, automated or manually controlled by the users.

Acknowledgments

This paper is part of a PhD study supported by the scholarship "Borsa per dottorandi di ricerca delle Universitá Milanesi" funded by Fondazione Fratelli Confalonieri. The authors thank Prof Claudio Del Pero (Politecnico di Milano) for valuable suggestions, and Florian Antretter and Daniel Zirkelbach (Fraunhofer Institut für Bauphysik) for helpful exchanges and for providing access to WUFI Plus. The authors also thankfully acknowledge the staff of Osservatorio Meteo Milano Duomo for the validation of weather data of the station at Politecnico di Milano.

Supplementary material

Appendix A:

The hybrid procedure of generating random samples from complex urban canyons is provided in Figure 13. In the flowchart, the range of each uncertain input parameter is indicated as X_i, while x_i refers to a random sample. Also, i counts the number of random generations in the probabilistic loop, while j counts the number of samples obtained from α-cuts. The final set of samples generated by hybrid treatment is highlighted as G_j^i , the size of which is equal to $i \times j$. The random samples associated with probabilistic uncertainty (see Table 1) are generated within Loop1. We used the Monte Carlo method to sample from probability distributions. Loop 2 approximates the possibilistic distributions of epistemic parameters (see Table 1).

A trapezoid possibility distribution function is devised to represent the epistemic uncertainty within the theory of possibility (Figure 14). The trapezoid's base edge represents the entire range of a parameter, while the top edge represents the most probable range of variation. In this study, the trapezoid possibility distribution function's shape is based on values reported in the literature (de Abreu-Harbich et al., 2015). The trapezoid is sliced in equal intervals to sample from the possibility distribution function. Each slice is known as an α-cut and defines a range of uncertainty, within which all values are equally plausible (Guyonnet et al., 2003). As displayed in Figure 2, we

applied three α-cuts to the trapezoid distribution, one at the base, one in the middle, and one at the top. As a result, 0 and 1 represent the base range (first α-cut), 0.1 and 0.7 form the middle slice (second α-cut), and lastly, 0.2 and 0.3 form the top edge of the distribution (third α-cut).

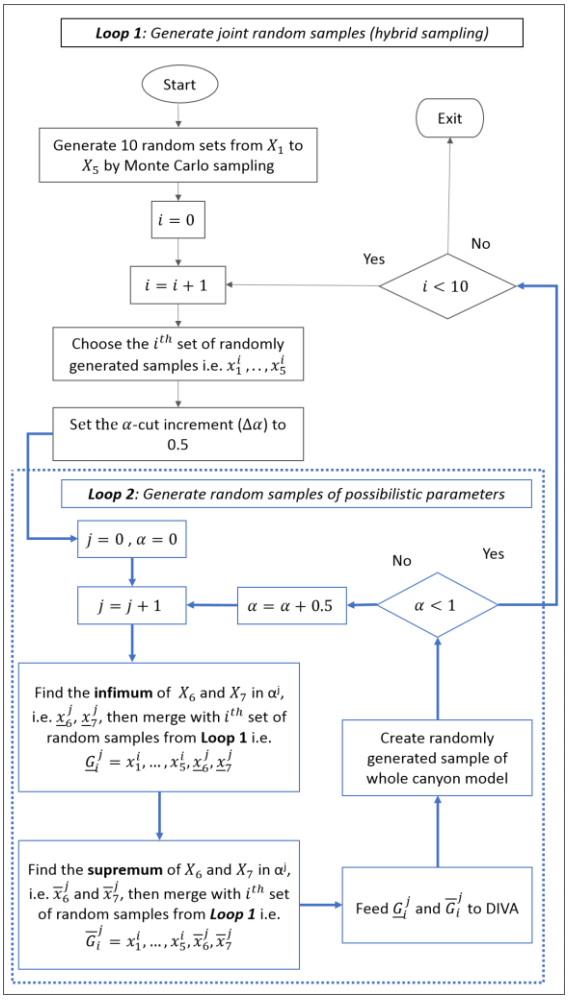

Figure 13- Hybrid approach framework, this flowchart is a customization of the proposed flowchart in (Khayatian et al., 2018).

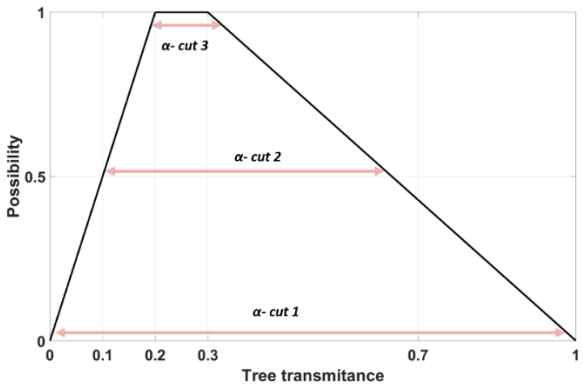

Figure 14. An illustration of a possibilistic representation of uncertainty (an example of tree transmittance).

Appendix B:

Details of uncertainty associated with urban canyon models

Table 4- A guide to generated samples for uncertainty associated scenarios; (*) is the actual diameter of the located tree in front of the studied area for glare.

Average values	G_1^j	G_2^j	G_3^j	G_4^j	G_5^j	G_6^j	G_7^j	G_8^j	G_9^j	G_{10}^j
Exterior wall reflectance (-)	0.30	0.40	0.42	0.35	0.31	0.41	0.32	0.44	0.35	0.40
WWR (%)	0.47	0.48	0.52	0.44	0.49	0.39	0.41	0.53	0.46	0.4
Height of adjacent buildings (m)	4.1	4	4	3.7	4.1	3.8	4	3.8	4	4
Trees crown dimeter* (m)	9	6.3	8.1	7.4	8.4	8.6	8.3	6.6	7.3	7.7

Each image corresponds to a random sample from aleatory uncertainties. The epistemic uncertainties in Figure 15 are fixed ($\overline{G}_i^2$, where Trans = 0.7), and all images correspond to 11 am on 22nd December. A more comprehensive view of all aleatory samples is provided in Appendix B-Table 4.

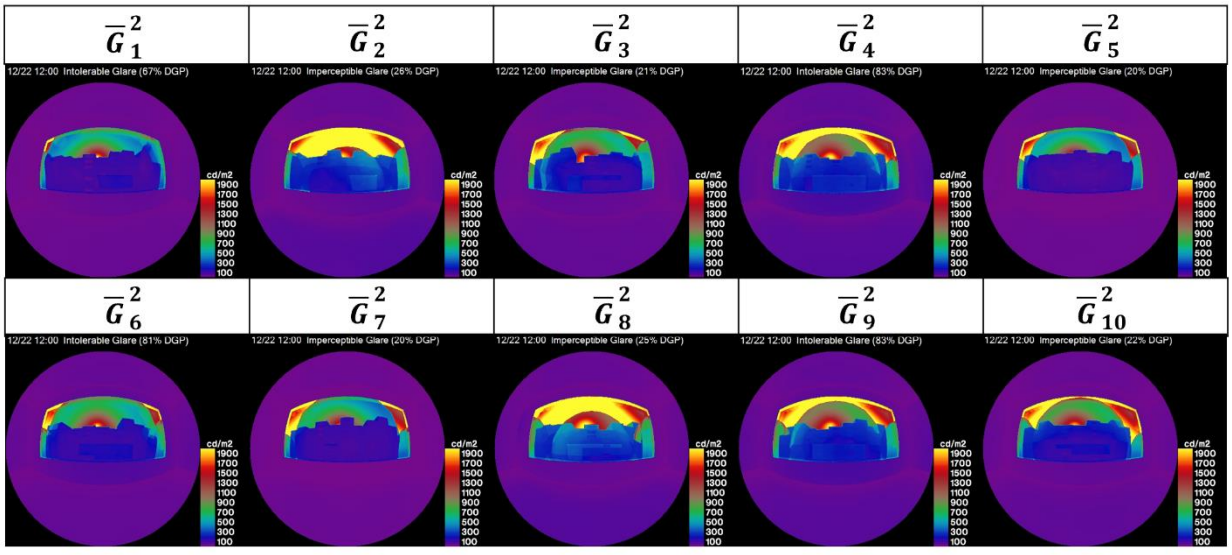

Figure 15 - Outside view of studied floor in all probabilistic samples with tree Trans=0.7 on December 22nd -12 pm with tree Trans = 0.7.

References

1. Al Horr, Y., Arif, M., Kaushik, A., Mazroei, A., Katafygiotou, M., Elsarrag, E., 2016. Occupant productivity and office indoor environment quality: A review of the literature. Build. Environ. https://doi.org/10.1016/j.buildenv.2016.06.001
2. Ali-Toudert, F., Mayer, H., 2006. Numerical study on the effects of aspect ratio and orientation of an urban street canyon on outdoor thermal comfort in hot and dry climate. Build. Environ. 41, 94–108. https://doi.org/10.1016/j.buildenv.2005.01.013
3. Andersen, M., 2015. Unweaving the human response in daylighting design. Build. Environ. 91, 101–117. https://doi.org/10.1016/j.buildenv.2015.03.014
4. Antoniadou, P., Papadopoulos, A.M., 2017. Occupants' thermal comfort: State of the art and the prospects of personalized assessment in office buildings. Energy Build. https://doi.org/10.1016/j.enbuild.2017.08.001
5. Antretter, F., Winkler, M., 2015. WUFI ® Plus 3.0 Manual.
6. Arens, E., Hoyt, T., Zhou, X., Huang, L., Zhang, H., Schiavon, S., 2015. Modeling the comfort effects of short-wave solar radiation indoors. Build. Environ. 88, 3–9. https://doi.org/10.1016/j.buildenv.2014.09.004
7. Balakrishnan, P., Jakubiec, J.A., 2016. Measuring Light Through Trees for Daylight Simulations: a Photographic and Photometric Method.
8. Berry, R., Livesley, S.J., Aye, L., 2013. Tree canopy shade impacts on solar irradiance received by building walls and their surface temperature. Build. Environ. https://doi.org/10.1016/j.buildenv.2013.07.009
9. Buratti, C., Palladino, D., Ricciardi, P., 2016. Application of a new 13-value thermal comfort scale to moderate environments. Appl. Energy 180, 859–866. https://doi.org/10.1016/j.apenergy.2016.08.043
10. Chatzidimitriou, A., Yannas, S., 2017. Street canyon design and improvement potential for urban open spaces; the influence of canyon aspect ratio and orientation on microclimate and outdoor comfort. Sustain. Cities Soc. 33, 85–101. https://doi.org/10.1016/j.scs.2017.05.019
11. Chen, J., Augenbroe, G., Wang, Q., Song, X., 2017. Uncertainty analysis of thermal comfort in a prototypical naturally ventilated office building and its implications compared to deterministic simulation. Energy Build. 146, 283–294. https://doi.org/10.1016/j.enbuild.2017.04.068
12. Chinazzo, G., Wienold, J., Andersen, M., 2019. Daylight affects human thermal perception. Sci. Rep. 9, 1–15.
13. Costanzo, V., Donn, M., 2017. Thermal and visual comfort assessment of natural ventilated office buildings in Europe and North America. Energy Build. 140, 210–223. https://doi.org/10.1016/j.enbuild.2017.02.003
14. Crone, S., 1992. Radiance users manual. Glass.
15. Curci, S., Lavecchia, C., Frustaci, G., Paolini, R., Pilati, S., Paganelli, C., 2017. Assessing measurement uncertainty in meteorology in urban environments. Meas. Sci. Technol. aa7ec1. https://doi.org/10.1088/1361-6501/aa7ec1
16. de Abreu-Harbich, L.V., Labaki, L.C., Matzarakis, A., 2015. Effect of tree planting design and tree species on human thermal comfort in the tropics. Landsc. Urban Plan. 138, 99–109. https://doi.org/10.1016/j.landurbplan.2015.02.008
17. Dubois, D., Prade, H., 2001. Possibility theory , probability theory and multiple- valued

logics : A clarification. Ann. Math. Artif. Intell. 32, 35–66. https://doi.org/10.1023/A:1016740830286
18. Fanger, P.O., others, 1970. Thermal comfort. Analysis and applications in environmental engineering. Therm. Comf. Anal. Appl. Environ. Eng.
19. Fraunhofer-Gesellschaft, 2019. Creating weather files [WWW Document]. URL https://wufi.de/en/service/downloads/creating-weather-files/
20. Gong, F.Y., Zeng, Z.C., Ng, E., Norford, L.K., 2019. Spatiotemporal patterns of street-level solar radiation estimated using Google Street View in a high-density urban environment. Build. Environ. 148, 547–566. https://doi.org/10.1016/j.buildenv.2018.10.025
21. Gong, F.Y., Zeng, Z.C., Zhang, F., Li, X., Ng, E., Norford, L.K., 2018. Mapping sky, tree, and building view factors of street canyons in a high-density urban environment. Build. Environ. 134, 155–167. https://doi.org/10.1016/j.buildenv.2018.02.042
22. Gronlund, C.J., Berrocal, V.J., 2020. Modeling and comparing central and room air conditioning ownership and cold-season in-home thermal comfort using the American Housing Survey. J. Expo. Sci. Environ. Epidemiol. 30, 814–823. https://doi.org/10.1038/s41370-020-0220-8
23. Guyonnet, D., Bernard Bourgine, ;, Dubois, ; Didier, Hé Lè Ne Fargier, ;, Cô Me, ; Bernard, Chilè, J.-P., Bourgine, B., Dubois, D., Fargier, H., Côme, B., Chilès, J.-P., 2003. Hybrid Approach for Addressing Uncertainty in Risk Assessments. J. Environ. Eng. 129, 68–78. https://doi.org/10.1061/(ASCE)0733-9372(2003)129:1(68)
24. Holm, A., Kuenzel, H.M., Sedlbauer, K., 2003. the Hygrothermal Behaviour of Rooms : Combining Thermal Building Simulation and Hygrothermal Envelope Calculation. Build. Simul. 499–506.
25. Hu, S., Hoare, C., Raftery, P., O'Donnell, J., 2019. Environmental and energy performance assessment of buildings using scenario modelling and fuzzy analytic network process. Appl. Energy 255, 113788. https://doi.org/10.1016/j.apenergy.2019.113788
26. Humphreys, M., Nicol, F., 2015. Enviromental Design: CIBSE Guide A. https://doi.org/10.1016/B978-0-240-81224-3.00016-9
27. Iwata, T., Taniguchi, T., Sakuma, R., 2017. Automated blind control based on glare prevention with dimmable light in open-plan offices. Build. Environ. 113, 232–246. https://doi.org/10.1016/j.buildenv.2016.08.034
28. Jakubiec, J.A., Reinhart, C.F., 2012. The 'adaptive zone'-A concept for assessing discomfort glare throughout daylit spaces. Light. Res. Technol. 44, 149–170. https://doi.org/10.1177/1477153511420097
29. Jamei, E., Rajagopalan, P., 2017. Urban development and pedestrian thermal comfort in Melbourne. Sol. Energy 144, 681–698. https://doi.org/10.1016/j.solener.2017.01.023
30. Khayatian, F., Meshkinkiya, M., Baraldi, P., Di Maio, F., Zio, E., 2018. Hybrid Probabilistic-Possibilistic Treatment of Uncertainty in Building Energy Models: A Case Study of Sizing Peak Cooling Loads. ASCE-ASME J. Risk Uncertain. Eng. Syst. Part B Mech. Eng. 4. https://doi.org/10.1115/1.4039784
31. Kiureghian, A. Der, Ditlevsen, O., 2009. Aleatory or epistemic? Does it matter? Struct. Saf. 31, 105–112. https://doi.org/10.1016/j.strusafe.2008.06.020
32. Ko, W.H., Schiavon, S., Brager, G., Levitt, B., 2018. Ventilation, thermal and luminous autonomy metrics for an integrated design process. Build. Environ.

https://doi.org/10.1016/j.buildenv.2018.08.038
33. Kotthaus, S., Smith, T.E.L., Wooster, M.J., Grimmond, C.S.B., 2014. Derivation of an urban materials spectral library through emittance and reflectance spectroscopy. ISPRS J. Photogramm. Remote Sens. 94, 194–212. https://doi.org/10.1016/j.isprsjprs.2014.05.005
34. Krayenhoff, E.S., Jiang, T., Christen, A., Martilli, A., Oke, T.R., Bailey, B.N., Nazarian, N., Voogt, J.A., Giometto, M.G., Stastny, A., Crawford, B.R., 2020. A multi-layer urban canopy meteorological model with trees (BEP-Tree): Street tree impacts on pedestrian-level climate. Urban Clim. 32, 100590. https://doi.org/10.1016/j.uclim.2020.100590
35. Kristl, Ž., Košir, M., Trobec Lah, M., Krainer, A., 2008. Fuzzy control system for thermal and visual comfort in building. Renew. Energy 33, 694–702. https://doi.org/10.1016/j.renene.2007.03.020
36. Krüger, E., Pearlmutter, D., Rasia, F., 2009. Evaluating the impact of canyon geometry and orientation on cooling loads in a high-mass building in a hot dry environment. Appl. Energy 87, 2068–2078. https://doi.org/10.1016/j.apenergy.2009.11.034
37. Kubaha, K., Fiala, · D, Toftum, · J, Taki, · A H, 2004. Human projected area factors for detailed direct and diffuse solar radiation analysis. Int J Biometeorol 49, 113–129. https://doi.org/10.1007/s00484-004-0214-6
38. La Gennusa, M., Nucara, A., Pietrafesa, M., Rizzo, G., 2007. A model for managing and evaluating solar radiation for indoor thermal comfort. Sol. Energy 81, 594–606. https://doi.org/10.1016/j.solener.2006.09.005
39. Lauzet, N., Rodler, A., Musy, M., Azam, M.-H., Guernouti, S., Mauree, D., Colinart, T., 2019. How building energy models take the local climate into account in an urban context – A review. Renew. Sustain. Energy Rev. 116, 109390. https://doi.org/10.1016/j.rser.2019.109390
40. Levinson, R., Pan, H., Ban-Weiss, G., Rosado, P., Paolini, R., Akbari, H., 2011. Potential benefits of solar reflective car shells: Cooler cabins, fuel savings and emission reductions. Appl. Energy 88, 4343–4357. https://doi.org/10.1016/j.apenergy.2011.05.006
41. Mao, J., Yang, J.H., Afshari, A., Norford, L.K., 2017. Global sensitivity analysis of an urban microclimate system under uncertainty: Design and case study. Build. Environ. 124, 153–170. https://doi.org/10.1016/j.buildenv.2017.08.011
42. Marino, C., Nucara, A., Pietrafesa, M., 2017. Thermal comfort in indoor environment: Effect of the solar radiation on the radiant temperature asymmetry. Sol. Energy 144, 295–309. https://doi.org/10.1016/j.solener.2017.01.014
43. Martins, T.A. de L., Adolphe, L., Bastos, L.E.G., Martins, M.A. de L., 2016. Sensitivity analysis of urban morphology factors regarding solar energy potential of buildings in a Brazilian tropical context. Sol. Energy 137, 11–24. https://doi.org/10.1016/j.solener.2016.07.053
44. Mohajeri, N., Gudmundsson, A., Kunckler, T., Upadhyay, G., Assouline, D., Kämpf, J.H., Scartezzini, J.-L., 2016. How street canyon configuration control the accessibility of solar energy potential: Implication for urban design, in: Proceedings of the 36th International Conference on Passive and Low Energy Architecture.
45. Mujan, I., Anđelković, A.S., Munćan, V., Kljajić, M., Ružić, D., 2019. Influence of indoor environmental quality on human health and productivity - A review. J. Clean. Prod. 217, 646–657. https://doi.org/10.1016/j.jclepro.2019.01.307
46. Nevat, I., Ruefenacht, L.A., Aydt, H., 2020. Recommendation system for climate informed urban design under model uncertainty. Urban Clim. 31.

https://doi.org/10.1016/j.uclim.2019.100524
47. Nundy, S., Ghosh, A., 2020. Thermal and visual comfort analysis of adaptive vacuum integrated switchable suspended particle device window for temperate climate. Renew. Energy 156, 1361–1372. https://doi.org/10.1016/j.renene.2019.12.004
48. Ole Fanger, P., Toftum, J., 2002. Extension of the PMV model to non-air-conditioned buildings in warm climates, in: Energy and Buildings. https://doi.org/10.1016/S0378-7788(02)00003-8
49. Ozcelik, G., Becerik-Gerber, B., Chugh, R., 2019. Understanding human-building interactions under multimodal discomfort. Build. Environ. 151, 280–290. https://doi.org/10.1016/j.buildenv.2018.12.046
50. Paolini, R., Zani, A., MeshkinKiya, M., Castaldo, V.L., Pisello, A.L., Antretter, F., Poli, T., Cotana, F., 2017. The hygrothermal performance of residential buildings at urban and rural sites: Sensible and latent energy loads and indoor environmental conditions. Energy Build. 152, 792–803. https://doi.org/10.1016/j.enbuild.2016.11.018
51. Perini, K., Magliocco, A., 2014. Effects of vegetation, urban density, building height, and atmospheric conditions on local temperatures and thermal comfort. Urban For. Urban Green. 13, 495–506. https://doi.org/10.1016/j.ufug.2014.03.003
52. Pierson, C., Sarey Khanie, M., Bodart, M., Wienold, J., 2019. Discomfort Glare Cut-Off Values From Field and Laboratory Studies 24, 295–305. https://doi.org/10.25039/x46.2019.op41
53. Ren, Z., Chen, D., 2018. Modelling study of the impact of thermal comfort criteria on housing energy use in Australia. Appl. Energy 210, 152–166. https://doi.org/10.1016/j.apenergy.2017.10.110
54. Salata, F., Golasi, I., de Lieto Vollaro, R., de Lieto Vollaro, A., 2016. Outdoor thermal comfort in the Mediterranean area. A transversal study in Rome, Italy. Build. Environ. 96, 46–61. https://doi.org/10.1016/j.buildenv.2015.11.023
55. Samaniego, E., Anitescu, C., Goswami, S., Nguyen-Thanh, V.M., Guo, H., Hamdia, K., Zhuang, X., Rabczuk, T., 2020. An energy approach to the solution of partial differential equations in computational mechanics via machine learning: Concepts, implementation and applications. Comput. Methods Appl. Mech. Eng. 362, 112790. https://doi.org/10.1016/j.cma.2019.112790
56. Solemma, L.L.C., 2014. DIVA for Rhino. Available.[accessed 27.06. 15].
57. Stagakis, S., Burud, I., Thiis, T., Gaitani, N., Panagiotakis, E., Lantzanakis, G., Spyridakis, N., Chrysoulakis, N., 2019. Spatiotemporal monitoring of surface temperature in an urban area using UAV imaging and tower-mounted radiometer measurements. 2019 Jt. Urban Remote Sens. Event 1–4. https://doi.org/10.1109/jurse.2019.8808958
58. Standard, A., 2010. Standard 55-2010, Thermal environmental conditions for human occupancy. Am. Soc. Heating, Refrig. Air Cond. Eng.
59. Strømann-Andersen, J., Sattrup, P.A., 2011. The urban canyon and building energy use: Urban density versus daylight and passive solar gains. Energy Build. 43, 2011–2020. https://doi.org/10.1016/j.enbuild.2011.04.007
60. Sun, Y., Heo, Y., Tan, M., Xie, H., Jeff Wu, C.F., Augenbroe, G., 2014. Uncertainty quantification of microclimate variables in building energy models. J. Build. Perform. Simul. 7, 17–32. https://doi.org/10.1080/19401493.2012.757368
61. Svensson, M.K., 2004. Sky view factor analysis - Implications for urban air temperature

differences. Meteorol. Appl. 11, 201–211. https://doi.org/10.1017/S1350482704001288
62. Teixeira, H., Gomes, M.G., Moret Rodrigues, A., Pereira, J., 2020. Thermal and visual comfort, energy use and environmental performance of glazing systems with solar control films. Build. Environ. 168. https://doi.org/10.1016/j.buildenv.2019.106474
63. The MathWorks, 2018. MATLAB and Statistics Toolbox.
64. Tregenza, P., Wilson, M., 2013. Daylighting: architecture and lighting design. Routledge.
65. Tsoka, S., Tolika, K., Theodosiou, T., Tsikaloudaki, K., Bikas, D., 2018. A method to account for the urban microclimate on the creation of "typical weather year" datasets for building energy simulation, using stochastically generated data. Energy Build. 165, 270–283. https://doi.org/10.1016/j.enbuild.2018.01.016
66. Ulpiani, G., Benedettelli, M., di Perna, C., Naticchia, B., 2017. Overheating phenomena induced by fully-glazed facades: Investigation of a sick building in Italy and assessment of the benefits achieved via model predictive control of the AC system. Sol. Energy 157, 830–852. https://doi.org/10.1016/j.solener.2017.09.009
67. Vu-Bac, N., Lahmer, T., Zhuang, X., Nguyen-Thoi, T., Rabczuk, T., 2016. A software framework for probabilistic sensitivity analysis for computationally expensive models. Adv. Eng. Softw. 100, 19–31. https://doi.org/10.1016/j.advengsoft.2016.06.005
68. Wienold, J., Christoffersen, J., 2006. Evaluation methods and development of a new glare prediction model for daylight environments with the use of CCD cameras. Energy Build. 38, 743–757. https://doi.org/10.1016/j.enbuild.2006.03.017
69. Yang, R., Zhang, H., You, S., Zheng, W., Zheng, X., Ye, T., 2020. Study on the thermal comfort index of solar radiation conditions in winter. Build. Environ. 167. https://doi.org/10.1016/j.buildenv.2019.106456
70. Yang, W., Moon, H.J., 2019. Combined effects of acoustic, thermal, and illumination conditions on the comfort of discrete senses and overall indoor environment. Build. Environ. 148, 623–633. https://doi.org/10.1016/j.buildenv.2018.11.040
71. Zomorodian, Z.S., Tahsildoost, M., 2017. Assessment of window performance in classrooms by long term spatial comfort metrics. Energy Build. 134, 80–93. https://doi.org/10.1016/j.enbuild.2016.10.018